DEVELOPMENT OF A NEW METHODOLOGY TO MEASURE CONTACT PRESSURE ALONG A THERMO-ELECTO-MECHANICAL INTERFACE

Mohammadreza Emami[1], Daniel Marceau[1], Martin Désilets[2]

[1]University Research Centre on Aluminium (CURAL) – Aluminium Research Center (REGAL) – University of Québec at Chicoutimi; 555 Boul. de l'Université; Chicoutimi (Québec), Canada, G7H 2B1
[2]University of Sherbrooke; 2500 Boul. de l'Université; Sherbrooke (Québec), Canada, J1K 2R1

Keywords: Thermo-Electro-Mechanical Interface, Contact Pressure Measurement, Sensor Design

Abstract

Contact pressure and temperature fields are two of the significant factors which affect the anodic and cathodic voltage drops of Hall-Héroult cell. Although, the temperature field has been measured using some capturing devices, the contact pressure distribution along the thermo-electro-mechanical (TEM) interfaces, such as cast iron/carbon, has never been measured. In this study, a new methodology is proposed to measure the contact pressure distribution along TEM interfaces. Furthermore, a new sensor device is developed. The functionality of the proposed methodology as well as the developed sensor is examined via an experimental test in laboratory, representing the real industrial thermo-electro-mechanical behavior of the contact between the collector bar and the cathode block.

Introduction

The transfer of heat and electricity between two surfaces in mechanical contact is of great importance, since it is present in many applications, such as spot-welding of sheet metals, electrodes in arc furnaces, electrical switches and relays, Hall-Héroult cell, etc. In these processes, a number of thermal and electrical resistances are present due to inherent imperfect contacts.

Contact pressure and, in some cases, interface temperature are among several process parameters which affect electrical and thermal contact resistances. Therefore, the optimization of the TEM processes necessitates a good understanding of phenomena occurring at the interface, *i.e.* contact pressure, heat variation, and voltage drop distribution. Despite several studies in this field to measure the temperature field and voltage drop using different sensors and/or methodology, the contact pressure distribution along the TEM interfaces has never been measured.

Problematic

The primary aluminium industry is characterized by high-energy consumption, which is typically more than 13000 kWh per ton of aluminium. According to statistical data of the International Aluminium Institute (IAI), the global annual production of aluminium in 2012 was more than 45 million tons [1], which requires more than 585 TWh of DC power. However, the growing demand for energy-saving in the world is pushing this industry to decrease its power consumption. The DC power consumption (W) is calculated by Eq. 1:

$$W = {2980 \times \bar{V}}/{CE} \quad \text{(kWh/t-Al)} \qquad (1)$$

where $\bar{V}$ is the average voltage drop of the cell in volts, and CE is the current efficiency of the electrolysis process. According to Eq. 1, there are two methods to reduce DC power consumption. One is to improve the current efficiency of the process and the other is to decrease the cell voltage. For a typical cell which operates at 4.0V and 92% of CE, the DC power consumption could be reduced by 324 kWh/t-Al if the cell voltage is decreased by only 0.1 V. Taking into account the North American annual production in 2012, which is about 4850 thousand tons (according to AIA's statistical data), and considering 0.0663 CAD/kWh as the cost of energy, the importance of this portion of the voltage drop reduction in saving cost of energy per year is about:

$$324 \text{ (kWh/ton)} \times 0.0663 \text{(CAD/kWh)} \times 4{,}850 \times 10^3 \text{ (ton)}$$
$$\cong 104 \text{ Million CAD}$$

It is well known that the cell voltage may be represented by the following factors:

$$V_{cell} = E_o + \eta_a + \eta_c + I.R_a + I.R_c + I.R_B \qquad (2)$$

where E_o , η_a , η_c , R_a , R_c , R_B , and I are theoretical decomposition voltage of Al_2O_3 in the bath (V), anodic overvoltage (V), cathodic overvoltage (V), anode resistance (Ω), cathode resistance (Ω), molten bath resistance (Ω), and the cell current (A), respectively. As the values of E_o , η_a , η_c are given for a specific cell, the cell voltage depends on the voltage drop of bath, anodes and cathodes. Due to the weak quality of contact, a reasonable portion of anode and cathode voltage drops occur at the cast iron to carbon interface.

Contact pressure and temperature fields are two important intervening factors that affect the voltage drop of TEM systems, *e.g.* cast iron to carbon interface. The lack of measured contact pressure data at the TEM interfaces is mostly due to the unavailability of the pressure measurement devices which are applicable to the solid-solid interface at high temperature, in a zone of high electrical current passage. This is the reason that in the development of TEM models, *e.g.* cathode (or anode) lining model, the magnitude of contact pressure was assumed to reach a predefined value (based on voltage drop) or was estimated through numerical modeling.

Previous work

The first efforts to study TEM interfaces, analytically and empirically, go back to 1960's (see [2], [3], [4], [5]). In an attempt to optimize cast iron thickness in the stub hole, Brooks and Bullough found that the electrical contact resistance is a function

of both temperature and contact pressure [6]. Sørlie and Gran proposed an apparatus to characterize the electrical contact resistance of the cathode material [7]. Their results showed a substantial drop in the electrical contact resistance with increasing contact pressure. With the objective of modeling the TEM contact interface better, a novel phenomenological constitutive model was developed and calibrated with smooth steel-smooth graphitized carbon by Richard *et al*. [8]. They reproduced the Sørlie and Gran's experimental setup to validate their modeling results. Goulet [9] was the first to develop a fully coupled TEM model based on the finite element toolbox FESh++ [10]. In a recent study by Jeddi *et al*. [11], a fully coupled parametric TEM model of a half carbon block was proposed to investigate the multi-physical behavior of a hexapod anode assembly.

Methodology

After investigating the different types of contact pressure measurement sensors and considering the principal characteristics of the TEM processes present in a Hall-Héroult cell (*e.g.* high temperature and electric current), a technique based on utilization of a strain-gauge was found to be the most effective and applicable method.

Taking into account the existing limitations in the fabrication of the available strain-gauges for contact pressure measurements which can be installed at the cast iron- carbon interface, without affecting the contact condition and withstanding high temperature (960˚C), it is decided to install the strain-gauge based sensor at a certain distance from the interface.

To position the sensor in the vicinity of the interface, a hole has to be drilled in one of the solids in contact. Carbon seems to be the best choice for this purpose due to its higher deflection under pressure, consequently resulting in a potentially stronger signal from the strain-gauge installed in such a material. Furthermore, considering the geometry of anode and cathode, carbon is more accessible than cast iron for the insertion of a sensor.

Based on such a design, the contact pressure from the interface is transferred to the sensor (strain-gauge) via intermediate solid. Subsequently, the sensor deforms under pressure (figure 1). The measured strain on the sensor is proportional to the contact pressure at the adjacent interface.
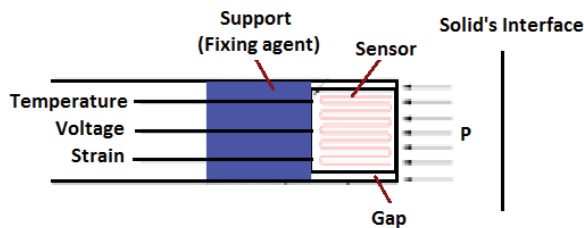

Figure 1: Sensor positioning inside the hole close to the interface

A thermocouple as well as a voltage probe are placed in the same position to quantify temperature and voltage in addition to the amount of strain. A fixation agent is used to prevent the sensor from sliding inside the hole.

By installing a number of sensors at a certain distance from the interface at several points, it is possible to determine the contact pressure distribution along the interface.

Design of the experimental setup

The schematic of the proposed setup for laboratory experiments is illustrated in figure 2.

As it is shown in this figure, two cylindrical samples are positioned vertically, one on top of the other. The strain-gauge based sensor is inserted inside a hole drilled in the bottom sample. The pressure is applied on the top of the upper sample via a lever mechanism in six loading steps. The maximum pressure applied is 5.5 MPa, which is an average value estimated from the numerical analysis done by Jeddi *et al.* [11]. The cylindrical samples are placed inside an oven designed to heat the test environment up to 1000˚C. Furthermore, an external source of current is employed to get a current density of 1 A/cm^2 through the samples, which represents the average current density at cast iron to carbon interface in a typical cathodic block (see [12]).

Repeating the loading at different pressures, temperatures, and current densities provides the calibration curve which gives the dependence of the measured strain on the applied contact pressure.

In an industrial electrolytic cell, where it is only possible to read strain signals, the use of such a calibration curve will be necessary to find the value of the contact pressure at the adjacent interface.
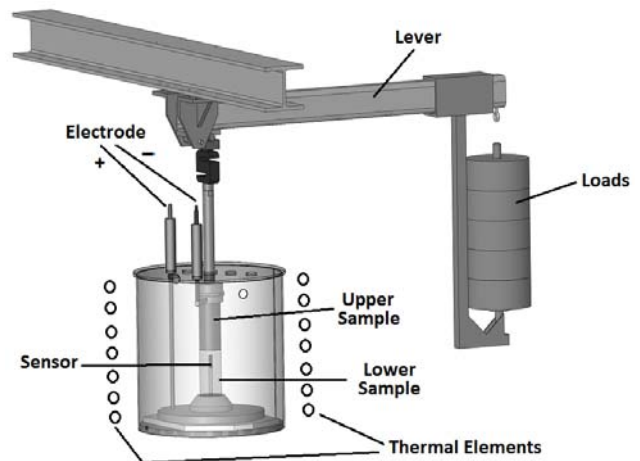

Figure 2: Proposed setup for the experiments

Material selection

Considering the fact that the main portion of anode and cathode voltage drops arises from the cast iron-carbon interface, the focus of material selection of samples was put on the cast iron and carbon materials. However, these two materials can have a large variety of compositions, even in a particular aluminium smelter. To minimize the negative effects of property variation due to composition changes, a commercial grade of steel and pure graphite were chosen as the sample materials.

The substrate is the deforming agent, on which the strain-gauge is placed, which is then inserted inside the graphite sample. The substrate material should have the capacity to adhere to the strain-gauge for higher temperature applications. The only method to join strain-gauge to the substrate which will resist at high temperatures is spot-welding. Therefore, the substrate material has

to be spot-weldable. Furthermore, this material needs to have high oxidation resistance, very low creep at high temperatures and close-to-carbon thermal expansion since it is placed inside the graphite sample and subjected to deformation due to the pressure. Considering the above mentioned properties, stainless steel 416 was chosen as the substrate material.

A high-temperature graphite-based glue is applied on a graphite back support to fix the sensor inside the hole.

The electric current (I) was applied through the samples, from the top. If the electric current passes through the sensor (*i.e.* strain-gauge), it will burn the strain-gauge circuits. To prevent this, alumina insulators were placed all around the sensor as illustrated in figure 3.
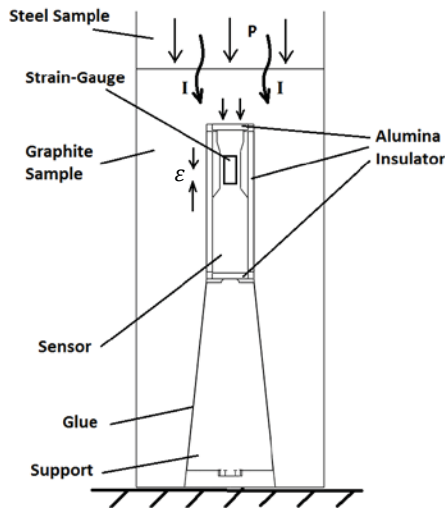

Figure 3: Full schematic of samples and sensor configuration

Sensitivity analysis

The principal objective of the sensitivity analysis, conducted via numerical modeling of the chosen concept, is to investigate the effects of intervening parameters on the stress/strain distribution inside the samples. This study will result in a better understanding of the behavior of the setup configuration. The outcomes of this analysis were used as a reference for the detailed design of the samples and sensor on the previously described experimental bench.

The academic research version of ANSYS® Workbench, release 14.0, was employed for the numerical modeling of the setup configuration. To perform the sensitivity analysis, a preliminary geometrical model has to be created for the samples and sensor. Investigating the sensitivity of this model to the intervening factors will result in an optimum geometry for the samples and sensor. The most important parameters in the creation of this geometrical model were the laboratory limitations and the size of available strain-gauges. The boundary conditions were applied to the model considering what was explained in the experimental setup conception and material selection.

The main controlling parameters in the sensitivity analysis are the risk of fracture in the graphite sample, the strain signal strength at the sensor's position and the contact pressure at the samples'

interface. Indeed, contact pressure distribution at the samples' interface should not be influenced by the insertion of the sensor inside the graphite sample. Moreover, the stress concentration inside the graphite sample due to the presence of the sensor should not cause any fracture in the graphite sample. Finally, the magnitude of strain at the sensor position should be large enough to be measured by a strain-gauge.

Among the most influencing parameters which could affect the above-mentioned controlling factors, one finds the sensor's diameter (or hole's diameter) and sensor's tip-to-interface distance. Figures 4 and 5 show the effect of these parameters on the stress distribution at samples' interface and on the measurable strain at the sensor's position, both of which are estimated via numerical modeling.

The normalized contact pressure is the ratio of contact pressure in the experiments when there is a sensor inside the graphite sample to that of the experiments with no sensor inside this sample. In other words, when the normalized value is close to one, the contact pressure at the interface is not affected by the presence of the sensor.
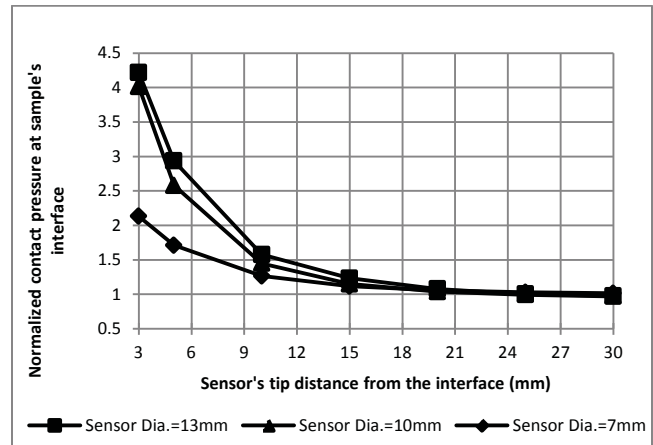

Figure 4: Effect of sensor's tip-to-interface distance and the sensor's diameter on the contact pressure at the samples' interface
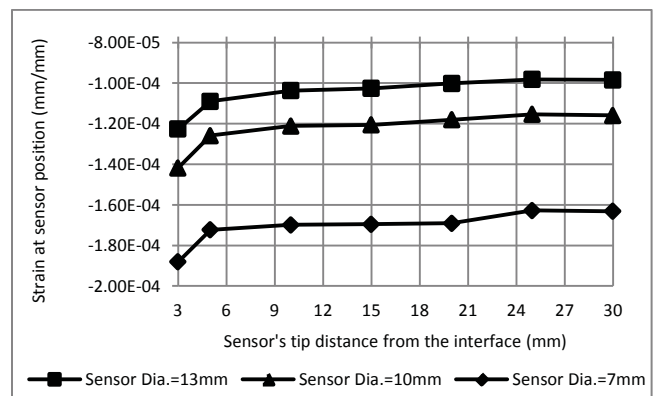

Figure 5: Effect of sensor's tip-to-interface distance and the sensor's diameter on the measurable strain at the sensor's position

It is obvious from figure 4, 5 that increasing the diameter of the sensor will increase the stress value at the samples' interface as compared with the condition when there is no sensor inside the

sample. At the same time, it decreases the magnitude of strain at the sensor's position.

Furthermore, it is shown that locating the sensor too close to the interface will have a higher effect on contact pressure at the interface. However, it increases the strain magnitude at sensor which makes it more sensitive. When the sensor's tip-to-interface distance is more than 15 mm, the value of the contact pressure at the samples' interface is almost uninfluenced.

On the other hand, based on the sensitivity analysis, it becomes clear that increasing the diameter of sensor, and consequently the hole size inside the graphite sample, has an important impact on the mechanical behavior of materials in its neighborhood. The diameter should be chosen as small as possible to minimize the stress concentration inside the graphite sample, and to avoid its fracture of graphite sample. A small tip-to-interface distance has the same negative effect.

According to the above-mentioned discussion, the sensor's diameter and the tip-to-interface distance are chosen to be 8 mm and 15 mm, respectively.

Results and discussion

Experiments have been conducted at room temperature on the setup configuration described in the previous section. However, the Joule effect generated by the passage of an electric current through the samples is responsible for the heat generation inside the sample as well as at the samples' interface.

The contact resistance dependency on the contact pressure is demonstrated in figure 6. At each loading step, the value of the electrical contact resistance is calculated by the same equations as described in Sørlie and Gran's work [7]. To calculate the electrical contact resistance using those equations, the value of voltage drop is obtained using two voltage probes in two sides of the interface. The results showed that there is a substantial drop in electric contact resistance as the contact pressure increases up to 3 MPa, after it stays almost constant. These results are in good agreement with those published by Sørlie and Gran [7]. The value of contact resistance is close to 0.5 Ωmm^2, when the contact pressure exceeds 5 MPa. The surface roughness of samples has an important effect on the value of contact resistance. In this study, the surface roughness of the samples' interface is close to Ra=6.4μm [13]. Increasing the roughness of samples' surfaces, will increase the value of contact resistance.
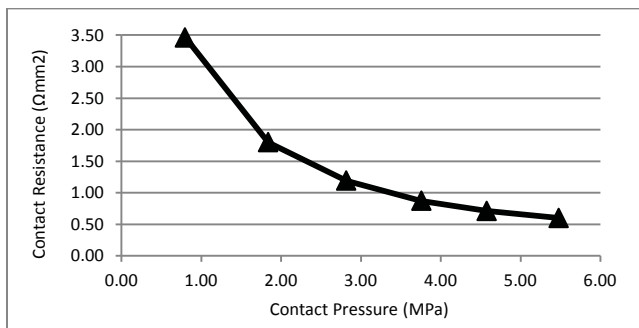

Figure 6: Contact resistance versus contact pressure at the samples' interface

Figures 7 and 8 present the most important outcomes of this study, which are the relation between strain measured by the sensor and contact pressure, and contact resistance, respectively.
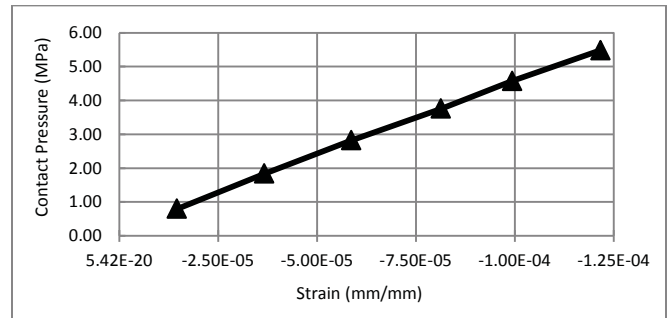

Figure 7: Contact pressure at samples' interface versus measured strain at sensor (calibration curve)

In fact, figure 7 is the calibration chart, which gives the value of the contact pressure as a function of the strain signal from the strain-gauge. The importance of this type of curve is clear for the industrial electrolytic cell, where the strain value can be measured using this sensor. Then, the contact pressure can be determined from the calibration curve. At a contact pressure of 5.5 MPa, the strain signal from strain-gauge is about 1.2×10^{-4} mm/mm. The amount of strain induced by a specific pressure is highly dependent on the configuration of the hole in the sample, and strain-gauge's characteristics, as well as material properties of graphite sample and substrate.

Similarly, figure 8 shows the relation between strain signal from the sensor and contact resistance. The contact resistance decreases significantly with increasing the strain value which is induced by contact pressure. This curve can be used to estimate the value of contact resistance at the interface directly from the measured strain, under the similar thermal and mechanical conditions.
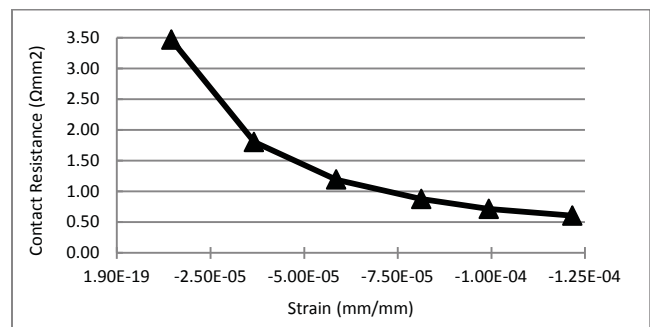

Figure 8: Contact resistance versus strain signal from sensor

The relation between contact pressure and interface temperature is illustrated in figure 9. At low contact pressures, the value of contact resistance at the interface of samples is high, which increases the heat generation via the Joule effect. However, increasing the contact pressure reduces the contact resistance, and interface temperature, consequently.
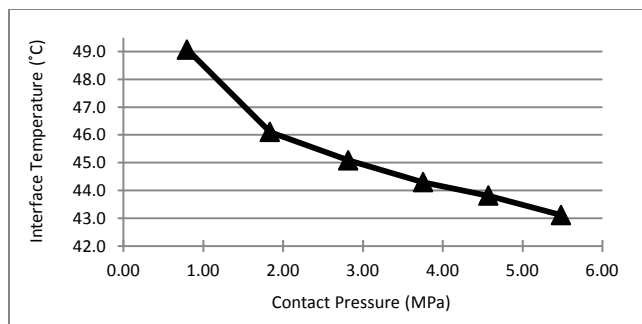
Figure 9: Interface heat generation versus contact pressure

Applicability at higher temperature

This paper is a proof of the concept developed for the utilization of a strain-gauge based sensor in the measurement of contact pressure along TEM interfaces. To be able to use this concept for measurement of the contact pressure at the cast iron-carbon interface in the aluminium electrolytic cell, it is necessary to modify the actual design further.

The most important modification required is related to the strain-gauge. It needs to be replaced by a higher temperature strain gauge. According to the authors of this paper, this type of strain-gauge is already available in the industry, such as "KHCX" model from Kyowa [14]. Also, an additional sensitivity analysis is required to adapt the dimensions of the samples and the sensor for its use inside an anode or a cathode block.

Conclusions

To the knowledge of authors, the value of contact pressure at a thermo-electro-mechanical interface has been measured for the first time via a strain-gauge based sensor.

During this study, a methodology that will lead a new way of investigating TEM processes, *e.g.* those found at carbon-cast iron interface inside the aluminium reduction cell, was developed. This methodology is based on the utilization of a calibration curve, which relates the strain signal obtained from the sensor to the contact pressure at a specific temperature.

The applicability of this methodology and strain-gauge based sensor is proved at room temperature on an experimental setup in the laboratory.

The future work will first focus on increasing the temperature up to 1000˚C, which is the maximum operating temperature in the aluminium electrolysis cell. This requires utilization of a number of higher temperature strain-gauges.

References

[1] "Primary Aluminium Production," 20 June 2013. [Online]. Available: http://www.world-aluminium.org/statistics/. [Accessed 20 June 2013].

[2] J. A. Greenwood, "Constriction resistance and the real area of contact," *British Journal of Applied Physics,* vol. 17, pp. 1621-1632, 1966.

[3] J. A. Greenwood and J. B. P. Williamson, "Contact of Nominally Flat Surfaces," in *Proceedings of the Royal Society of London*, 1966.

[4] R. Holm, Electric Contacts, Theory and Applications, 4th ed., New York: Springer, 1967.

[5] M. G. Cooper, B. B. Mikic and M. Yovanovich, "Thermal contact conductance," *International Journal of Heat and Mass Transfer,* vol. 12, no. 3, pp. 279-300, 1969.

[6] D. Brooks, V. Bullough, "Factors in the design of reduction cell anodes," *Pros. of TMS Light Metals,* pp. 961-976, 1984.

[7] M. Sørlie, H. Gran, "Cathode collector bar-to-carbon contact resistance," *Pros. of TMS Light Metals,* pp. 779-787, 1991.

[8] D. Richard, M. Fafarda, R. Lacroixa, P. Cléry, Y. Maltais, "Thermo-Electro-Mechanical modelling of the contact between steel and carbon cylinders using the finite element method," *Pros. of TMS Light Metals,* pp. 523-528, 2000.

[9] P. Goulet, "Modélisation du comportement thermo-électro-mécanique des interfaces de contact d'une cave de Hall-Héroult," Québec, Canada, 2004.

[10] M. Désilets, D. Marceau, M. Fafard, "START-Cuve: Thermo-electro-mechanical Transient Simulation Applied to Electrical Preheating of a Hall-Héroult Cell," *Pros. of TMS Light Metals,* pp. 247-254, 2003.

[11] E. Jeddi, D. Marceau, L. Kiss, L. St-Georges, D. Laroche, L. Hacini, "Experimental and numerical investigation of voltage drop in anode assemblies," *Pros. of TMS Light Metals,* pp. 1347-1352, 2013.

[12] M. Blais, M. Désilets, M. Lacroix, "Energy saving in aluminum electrolysis cells: effect of the cathode design," *Light Metals,* pp. 627-631, 2013.

[13] "Surface Texture (Surface Roughness, Waviness, and Lay)," ASME B46.1-2009, p. 120.

[14] "Encapsulated strain gages," Kyowa, [Online]. Available: http://www.kyowa-ei.co.jp/eng/product/strain_gages/gages/khcx.html. [Accessed 15 10 2013].